Published in final edited form as:
Stem Cells. 2008 August ; 26(8): 2104–2113. doi:10.1634/stemcells.2008-0115.

Fate-Mapping Evidence that Hepatic Stellate Cells are Epithelial Progenitors in Adult Mouse Livers

Liu Yang[1,*], **Youngmi Jung**[1,*], **Alessia Omenetti**[1], **Rafal P. Witek**[1], **Steve Choi**[1], **Hendrika M Vandongen**[1], **Jiawen Huang**[1], **Gianfranco D. Alpini**[2], and **Anna Mae Diehl**[1]

[1]Divisions of Gastroenterology, Duke University, Durham, NC, USA

[2]Research, Central Texas Veterans Health Care System, Scott & White and Texas A&M Health Science Center, College of Medicine, Temple, TX, USA

Abstract

Liver injury activates quiescent (Q) hepatic stellate cells (HSC) to proliferative, myofibroblasts (MF). Accumulation of MF-HSC sometimes causes cirrhosis and liver failure. However, MF-HSC also promote liver regeneration by producing growth factors for oval cells, bipotent progenitors of hepatocytes and cholangiocytes. Genes that are expressed by primary HSC isolates overlap with those expressed by oval cells, and hepatocytic and ductular cells emerge when HSC are cultured under certain conditions. We evaluated the hypothesis that HSC are a type of oval cell and, thus, capable of generating hepatocytes to regenerate injured livers. Because Q-HSC express glial fibrillary acidic protein (GFAP), we crossed mice in which GFAP promoter elements regulated Cre-recombinase with ROSA-loxP-stop-loxP-GFP mice to generate GFAP-Cre/GFP double transgenic mice. These mice were fed methionine choline deficient, ethionine supplemented (MCDE) diets to activate and expand HSC and oval cell populations. GFP(+) progeny of GFAP-expressing precursors were characterized by immunohistochemistry. Basal expression of mesenchymal markers was negligible in GFAP(+)Q-HSC. When activated by liver injury or culture, HSC down-regulated expression of GFAP but remained GFP(+); they became highly proliferative and began to co-express markers of mesenchyme and oval cells. These transitional cells disappeared as GFP-expressing hepatocytes emerged, began to express albumin, and eventually repopulated large areas of the hepatic parenchyma. Ductular cells also expressed GFAP and GFP, but their proliferative activity did not increase in this model. These findings suggest that HSC are a type of oval cell that transitions through a mesenchymal phase before differentiating into hepatocytes during liver regeneration.

Keywords

liver regeneration; stem cells; epithelial-mesenchymal transitions; hepatic stellate cells; glial fibrillary acidic protein

Introduction

The role of hepatic stellate cells in liver repair is being reconsidered because of growing evidence that these cells express certain stem cell markers [1–3], and produce various trophic factors for liver epithelial cells [4–8]. It is generally acknowledged that hepatic stellate cell

Corresponding Author: Anna Mae Diehl, M.D., Florence McAlister Professor & Chief, Division of Gastroenterology, Snyderman Building (GSRB-1) Suite 1073, 595 LaSalle Street, Duke University, Durham, North Carolina 27710, Tel: 919-684-4173, Fax: 919-684-4183, annamae.diehl@duke.edu.

*Equally contribute to this work as first authors

(HSC) populations in adult livers are heterogeneous [9, 10]. In healthy livers, quiescent (Q) HSC store vitamin A and other lipids [11–13]. They localize between sinusoidal endothelial cells and hepatocytes in the space of Disse. Chronic liver injury activates resident HSC to a proliferative, myofibroblastic (MF) phenotype. MF-HSC synthesize alpha smooth muscle actin (α-SMA) and are contractile. They also produce extracellular matrix molecules, such as type 1 collagen. Because portal hypertension, liver fibrosis, and sometimes cirrhosis, ensue when populations of MF-HSC expand, the transition of Q-HSC to MF-HSC is thought to portend a bad outcome in liver injury [9, 14, 15].

Other evidence, however, suggests that HSC may support regeneration of damaged livers. For example, HSC have been localized in canals of Hering, the stem cell niche in adult livers [16–18]. In addition, they are known to produce morphogens, including hepatocyte growth factor, epimorphin, pleiotrophin, and Hedgehog ligands [4–8]. In embryos and neonates, stellate cells may be important for the development of the intrahepatic biliary tree [19]. The trophic paracrine interactions between HSC and cholangiocytes persist into adulthood, as evidenced by reports that conditioned medium from adult HSC promotes the growth of cholangiocyte cell lines [20]. Therefore, it seems likely that in addition to remodeling matrix, HSC play a larger role in adult liver repair.

The minority opinion even posits that HSC may be progenitors for liver epithelial cells. This argument is based on data that Q-HSC from adults express markers of all three embryonic germ layers, such as glial fibrilary acidic protein (GFAP, an ectodermal marker) [21–23], desmin (a mesodermal marker) [24] and Hes-1(an endodermal marker)[25], as well as various stem cell markers, including nestin, CD105, p75 neurotrophin receptors, c-kit, and CD133 [1–3, 26, 27]. Recent cell culture findings support the plasticity of HSC by showing that Q-HSC are capable of differentiating into cell types other than MF[1]. For example, both primary rat HSC[1] and rat HSC lines that were clonally derived from primary rat HSC [7] differentiate into myofibroblastic, hepatocytic, bile ductular, or endothelial-like cells depending on the *in vitro* conditions. The opposing view, however, argues that the apparent multi-potency of HSC isolates resulted from the outgrowth of rare other cell types that contaminated the initial cell preparations. The same logic would confound interpretation of studies in which HSC isolates are transplanted into recipients in order to assess the role of HSC progeny in liver repair.

Fate mapping approaches overcome the inherent limitations of working with isolated cells and thus, are widely used to investigate cell fate during embryogenesis [28]. Therefore, we used this strategy to evaluate the fate of Q-HSC following liver injury. In order to mark Q-HSC and their progeny, we crossed transgenic mice in which GFAP promoter elements regulate Cre recombinase expression with other transgenic mice bearing floxed repressor alleles that control expression of green fluorescent protein (GFP) to generate double transgenic GFAP-Cre/GFP mice. In the double transgenic strain, progeny of GFAP-expressing Q-HSC are identified by expression of the marker gene (GFP) which persists even after GFAP gene expression has become down-regulated. Therefore, it is possible to determine if types of cells that do not normally express GFAP, such as hepatocytes and fibroblasts [21–23], are derived from Q-HSC. In humans, many types of chronic liver injury activate Q-HSC to myofibroblasts and induce expansion and differentiation of liver progenitors to replace dead mature hepatocytes [29–31]. Because chronic ingestion of methionine choline deficient, ethionine-supplemented (MCDE) diets are known to cause HSC activation and liver repopulation by progenitors in rodents [32–34], we fed GFAP-Cre/GFP mice and controls (GFP-floxed mice) MCDE diets to model the pathophysiology that occurs clinically.

We found that liver sinusoids of healthy adult GFAP-Cre/GFP mice were lined by stellate-appearing cells that expressed GFAP, GFP and Cre-recombinase. As expected, ingestion of MCDE diets provoked liver injury and fibrogenesis, and complete recovery from liver damage eventually occurred after the hepatotoxic diets were discontinued. Liver samples were obtained at different time points during this process and the fate of GFAP(+) Q-HSC was investigated using immunohistochemistry. Changes in gene expression profiles of primary HSC were also evaluated by QRT-PCR and Western blot analysis of samples obtained during culture-induced activation. Our results support the concept that Q-HSC are capable of functioning as multipotent progenitors, and can give rise to hepatocytes in adult livers.

Material and Methods

Animal model of liver injury

GFAP-Cre mice [35] and two strains of reporter mice, ROSA-loxP-stop-loxP-GFP [36] and ROSA-loxP-stop-loxP-LacZ [37], were obtained from Jackson Laboratories (Bar Harbor, ME). Mice expressing Cre recombinase under the control of GFAP regulatory elements (GFAP-Cre mice) were crossed with transgenic mice in which LoxP sites flanked a stop codon that repressed expression of reporter genes that encode either green fluorescent protein (GFP) (LoxP-GFP mice) or LacZ (LoxP-LacZ mice). In GFAP-Cre/LoxP-reporter double transgenic mice (hereafter referred to as GFAP-Cre/GFP mice and GFAP-Cre/LacZ mice), GFAP promoter elements drive expression of Cre recombinase to generate active enzyme that then removes the stop codon that is flanked by LoxP sites, thereby permitting expression of the marker genes (GFP or LacZ). Hence, in any cell (that at any time) activates GFAP expression, Cre recombinase is generated and this, in turn, results in an event (removal of the Lox P-flanked repressor element) that unleashes the ability to express the marker genes, GFP or LacZ. This strategy permits identification not only of cells that are actively expressing GFAP, but also of GFAP-negative cells that are descendents (progeny) of GFAP-expressing precursors which “passed” the capability of expressing GFP or LacZ to their daughters.

Preliminary studies demonstrated that LoxP-GFP and LoxP-LacZ mice had normal appearing livers and that HSC from these mice displayed typical culture-related induction of myofibroblastic genes. Therefore, since reporter gene expression is silenced in LoxP-GFP and LoxP-LacZ mice, we used these mice as controls (Ctr) in all subsequent experiments. In contrast, reporter gene expression is evident in GFAP-expressing cells and their progeny in GFAP-Cre/-Cre/GFP or GFAP-Cre/LacZ double transgenic (TG) mice).

All mice were housed in a facility with a 12-h light/dark cycle and allowed free access to food and water. Adult mice were used between 3 and 4 months of age. To induce oxidative liver injury, inhibit replication of mature hepatocytes, and activate HSC and liver progenitor populations, GFAP-Cre/GFP mice (n = 15) were fed methionine/choline-deficient diet supplemented with 0.15% ethionine (MCDE) [38–42]. Surviving mice were sacrificed after being fed MCDE diets for either 1 week (n = 4) or 3 weeks (n = 4). Another group of GFAP-Cre/GFP mice that were fed MCDE for 3 weeks (n = 4) were switched back to normal diet for another 3 weeks to allow liver recovery, and then sacrificed. Chow-fed GFAP-Cre/LacZ mice (n = 4) were also sacrificed to obtain tissue for localization of β-galactosidase activity.

Animal care and surgical procedures were approved by the Duke University Medical Center Institutional Animal Care and Use Committee as set forth in the “Guide for the Care and Use of Laboratory Animals” published by the National Institutes of Health.

Cell Isolation and culture

Hepatic stellate cells (HSC) were isolated from mice as previously described [43]. Briefly, after *in situ* perfusion of the liver with pronase (Boehringer Mannheim, Indianapolis, IN) followed by collagenase (Crescent Chemical, Hauppauge, NY), dispersed cell suspensions were layered on a discontinuous density gradient of 8.2% and 15.6% Accudenz (Accurate Chemical and Scientific, Westbury, NY). The resulting upper layer consisted of > 95% stellate cells, as defined by morphology and vitamin A-autofluorescence. The viability of all cells was verified by phase contrast microscopy as well as the ability to exclude propidium iodide. The viability of all cell cultures utilized for study was >95%. Isolated stellate cells were seeded at a density of 3 $X10^2$ cells/mm^2 with DMEM supplemented with 10% fetal bovine serum, 100 units/mL streptomycin and 100 units/mL penicillin.

Rat cholangiocytes were isolated as described as before [44], and kindly provided by Dr. Gianfranco Alpini (Texas A&M University).

mRNA Quantification by Real-Time RT-PCR

mRNAs were quantified by real-time RT-PCR per the manufacturer's specifications (Eppendorf, Mastercycler Real-Time PCR). The sequences of primers for mouse 18S, collagen I α1, α-SMA, GFAP, PPARγ, Aquaporin-1 (AQP), NCAM, MPK, CK7, EGFP, CK19 and AFP were as follows: 18S: sense: 5′-TTGACGGAAGGGCACCACCAG-3′, antisense : 5′-GCACCACCACCCACGGAATCG-3; collagen I α1: sense: 5′-GAGCGGAGAGTACTGGATCG-3′, antisense: 5′-GCTTCTTTTCCTTGGGGTTC-3′,α-SMA: sense: 5′-AAACAGGAATACGACGAAG-3′, antisense: 5′-CAGGAATGATTTGGAAAGGA-3′; GFAP: Sense: 5′-GCTTCCTGGAACAGCAAAAC-3′, antisense: 5′-ATCTTGGAGCTTCTGCCTCA-3′; PPARγ: sense: 5′-CACAATGCCATCAGGTTTGG-3′, antisense : 5′-GCTGGTCGATATCACTGGAGATC-3′; Aquaporin-1 : sense : 5′-GCTGGTCCAGGACAACGTG-3′,antisense: 5′-CCGCAGCCAGTGTAGTCAAT-3′; NCAM: sense: 5′-GACGTCCGGTTCATAGTCCT-3′, antisense : 5′-GGCAGTGGCATTCACGA-3′; MPK: sense: 5′-GCGTGTAGTGCCTGTACCTT-3′, antisense: 5′-GTAGGGCCCTGAATAATAGCTG-3′; CK7: sense: 5′-TAGAGTCCAGCATCGCAGAG-3′, antisense: 5′-CACAGGTCCCATTCCGTC-3′; EGFP: Sense: 5′-ACGTAAACGGCCACAAGTTC-3′, antisense: 5′-AAGTCGTGCTGCTTCATGTG-3′; CK19: sense: 5′-GTGAAGATCCGCGACTGGT-3′, antisense: 5′-AGGCGAGCATTGTCAATCTG-3′; AFP: Sense: 5′-GGTCGCTGGATCTCTAGGCT-3′, antisense: 5′-GCGGAAAGTCTCTCGGTCT-3′.

Total RNA was extracted from cells or whole livers using TRIzol (Invitrogen, Carlsbad, CA). One μg of RNA was reverse-transcribed using random primer and Superscript RNase H-reverse transcriptase (Invitrogen, Carlsbad, CA). Samples were incubated at 20° C for 10 minutes, 42° C for 30 minutes; reverse transcriptase was inactivated by heating at 99° C for 5 minutes and cooling at 5° C for 5 minutes. Amplification reactions were performed using a SYBR Green PCR Master Mix (Applied Biosystems). Fiveμl of diluted cDNA samples (1 to 5 dilution) were used for quantitative two-step PCR (a 10-minute step at 95° C, followed by 50 cycles of 15 seconds at 95° C and 1 minute at 65° C) in the presence of 400 nM specific forward and reverse primers, 5 mM MgCl2, 50 mM KCl, 10 mM Tris buffer (pH 8.3), 200 μM dATP, dCTP, dGTP, and 400 μM dUTP and 1.25 U of AmpliTaq Gold DNA polymerase (Perkin Elmer Applied Biosystems). Each sample was analyzed in triplicate. Target gene levels in treated cells or tissues are presented as a ratio to levels detected in corresponding control cells or tissues, according to the $^{\Delta\Delta}$Ct method.

Western blot analysis

Protein lysates were also prepared from the aforementioned HSC cultures and analyzed by immunoblot analysis as described[8]. Blots were incubated with primary antisera to either GFAP (1:1000, Santa Cruz, Santa Cruz, CA), a mesenchymal marker, α-sma (1:1000, Sigma, St. Louis, MO), and an epithelial marker, cytokeratin (CK)-7 (1:1000, Santa Cruz, Santa Cruz, CA). The expression of β-actin (Sigma, St. Louis, MO), a constitutively expressed housekeeping protein, was used as a loading control.

Immunohistochemistry

Specimens fixed in formalin and embedded in paraffin were cut into 4μm sections, dewaxed, hydrated, subsequently incubated for 10 min in 3 % hydrogen peroxide to block endogenous peroxidase. Antigen retrieval was performed by heating in 10mM sodium citrate buffer (pH 6.0) for 10 min or incubation with 0.25% pepsin for 10 min. Sections were blocked in Dako protein block (X9090;Dako) for 30 min and incubated with primary antibodies, GFP (ab6556, 1:2500; Abcam Ltd), GFAP (M0334, 1:4000; Dako), cre (69053-3, 1:10000; Novagen, La Jolla/ CA/USA), α-smooth muscle actin (M0851, 1:1000; Dako), Ki-67 (ab15580, 1:1000; Abcam Ltd), and AE1/3 (18-0132,1:500; Invitrogen) at room temperature 2 hours. Other sections also incubated at room temperature 2 hours in nonimmune sera. Polymer-HRP anti-rabbit (K4003; Dako) or anti-mouse (K4001;Dako) were used as secondary antibody. DAB reagent was employed in the detection procedure. Omitting primary antibodies from the reactions eliminated staining, demonstrating staining specificity.

For immunofluorescent staining, cells were fixed, permeabilized, and processed for immunostaining with primary antibody GFAP (1:1000, Calbiochem). Alexa Fluor 488 (Molecular Probes) was used as secondary antibodies. For double immunohistochemical staining, frozen liver sections were used. Samples were fixed and permeabilized, saturated, and processed for immunostaining with primary antibody GFP (ab6556) and albumin (MAB1455; 1:100; R&D Systems). Alexa Fluor 568 and Alexa Fluor 488 (Molecular Probes) were used as secondary antibodies. DAPI counterstaining was employed to demonstrate nuclei. To quantify Ki67 and GFP staining, seven PT and CV areas were randomly selected/section at 40X for each mouse. PT selected for analysis contained a portal vein that ranged from 130–180μm. The average number of Ki67 or GFP- positive cells was obtained by dividing the total number of positive cells by the total number of cells around the PT or CV.

Anonymized liver sections were also examined from three patients without chronic liver disease who had liver resections for colorectal metastases. Tissues were obtained from the Duke University School of Medicine Tissue Bank Shared Resource and studied in accordance with NIH and Institutional guidelines for human subject research.

Double immuno-staining

To determine if expression of certain proteins co-localized in cells, formalin-fixed/paraffin-embedded mouse liver sections were double immunostained for GFP and α-SMA, α-SMA and the S phase marker, Ki-67, and GFP and the liver epithelial progenitor marker, AE1/AE 3. Polymer-HRP anti-rabbit (K4003; Dako) and MACH3 mouse AP polymer kit (MP530, Biocare medical) were used as secondary antibodies. In each double immunostaining experiment, GFP or Ki67 was identified by DAB (Dako) to generate a brown color and each of the other markers was identified by Ferangi Blue chromogen kit (FB812S, Biocare Medical) that generated a blue color. De-identified, double-stained sections were examined by two independent observers who counted the numbers of single and double-positive cells in 7 fields/section/mouse under X40 magnification. Inter-observer variability was negligible.

Mean +/− SEM results are presented as # double(+) cells/field. To determine if GFAP expression co-localized with CK-7, a marker of immature biliary epithelial cells, frozen human liver sections were co-stained to demonstrate GFAP (M0334, 1:4000; Dako) and CK-7 (M7018, 1:750; Dako). Alexa Fluor 568 and Alexa Fluor 488 (Molecular Probes) were used as secondary antibodies. DAPI counterstaining was employed to demonstrate nuclei. Bile ductules comprised of double-positive cells were identified and photographed under X63 magnification.

Analysis of lacZ Expression

For qualitative analysis of lacZ expression, fixed tissues were stained by LacZ Detection Kit for Tissues (InvivoGen, San Diego, CA) according to the manufacturer's instruction.

Statistical Analysis

Results are expressed as mean ± SEM. Significance was established using the student's *t*-test and analysis of variance when appropriate. Differences were considered significant when $p < 0.05$.

Results

Liver sinusoids of healthy adult control mice (Fig 1A) and GFAP-Cre/GFP mice (Fig 1D) were lined by stellate-appearing cells that expressed GFAP. In GFAP-Cre/GFP mice, expression of GFP and Cre-recombinase were similarly localized (Fig 1E, F). Control mice did not exhibit expression of GFP or Cre-recombinase (Fig 1B, C). The staining characteristics of Q-HSC in GFAP-Cre/GFP mice suggested that these mice would be useful for tracking the progeny of Q-HSC. Unexpectedly, however, expression of GFAP (Fig 2A), Cre-recombinase (Fig 2B) and GFP (Fig 2C) were also demonstrated in bile duct cells and ductular appearing cells in peri-portal Canals of Hering in GFAP-Cre/GFP mice. A number of experiments were done to determine if ductular cell expression of these markers was artifactual. First, additional GFAP-Cre recombinase mice were crossed with mice harboring floxed-LacZ alleles to generate double transgenic GFAP-Cre/LacZ mice. β-galactosidase staining confirmed that intrahepatic and extrahepatic bile ducts of these GFAP-Cre/LacZ mice were derived from GFAP(+) cells (Fig 2D, E). The biliary tree in control mice exhibited no β-galactosidase activity (Fig 2F), confirming the specificity of this approach for detecting LacZ expression. Second, immunohistochemistry was used to demonstrate ductular cell staining for GFAP in non-diseased liver sections from healthy control mice (Fig 2G) and patients who were undergoing resection of metastatic colorectal cancers ((Fig 2H). In patients, frozen liver sections were also co-stained for both GFAP and CK-7, a marker of bipotent liver epithelial progenitors and immature biliary epithelial cells. Bile ductules comprised of GFAP/CK-7 double-positive epithelial cells were demonstrated by immunoflorescence microscopy (Supplemental material, Fig 1). Finally, expression of GFAP was demonstrated at the RNA level in freshly isolated primary cholangiocytes and HSC, but not hepatocytes, from healthy adult rats (Fig 2I). Thus, contrary to current dogma [21–23], Q-HSC are not the only type of cell that expresses GFAP in adult livers. In several species, ductular cells also express this marker. Hence, Q-HSC, ductular cells, and their progeny are all specifically marked by GFP in GFAP-Cre/GFP mice.

To evaluate the effects of liver injury on the GFAP(+) cell populations, GFAP-Cre/GFP mice were fed MCDE diets. Some mice were sacrificed one or three weeks later. Others were withdrawn from the MCDE diets at the three week time point and placed back on normal chow diets for an additional 3 weeks before being sacrificed. Ingestion of MCDE diets provoked liver injury and fibrogenesis, as evidenced by increased serum aminotransferase levels (Fig 3A), hyperbilirubinemia (Fig 3B), up-regulation of matrix gene

expression (Fig 3C), and loss of liver mass (Fig 3D). However, complete recovery from liver damage eventually occurred after the hepatotoxic diets were discontinued (Fig 3A–D). Liver sections were obtained from mice that had been fed the diets for either 1 or 3 weeks, and from mice that had been fed MCDE diets for 3 weeks and then returned to normal chow. IHC was done to track changes in the populations of cells that expressed GFAP and Cre-recombinase (Supplemental Fig 2). Results in the groups that had been fed MCDE diets were also compared to findings in healthy transgenic mice before exposure to MCDE diets (Fig 1D–F and 2 A–C). Bile ductular cells expressed both GFAP and Cre-recombinase before (Fig 2AC), during (Suppl Fig 2 A–D) and after (Suppl Fig 2E–F) MCDE-diet exposure, whereas GFAP+ve sinusoidal cells were noted only in mice with healthy livers (Fig 2). Mature-appearing hepatocytes were not noted to be GFAP+ve in any of the groups at any of the time points that were evaluated.

Changes in populations of cells that were derived from GFAP+ve cells (i.e., GFP-expressing cells) were assessed in the same animals (Fig 4). After one week of exposure to the hepatotoxic diets, the number of GFP+ve cells in portal tracts was similar to that of healthy livers, however large numbers of GFP+ve cells had accumulated in hepatic sinusoids (Fig 4A, B). Accumulation of GFP+ve, fibroblastic-appearing sinuosidal cells was particularly prominent in perivenular and midzonal areas (acinar zones 3 and 2) (Fig 4A). Occasional hepatocytic-appearing cells in these areas also expressed GFP (Fig 4B) at this time point. After 3 weeks of MCDE diet treatment, GFP-staining had become localized closer to portal tracts (Fig 4C). Hepatocytic cells were the predominant GFP+ve cell type in these areas (Fig 4D). Mice that had been withdrawn from MCDE diets and allowed to recover for a 3 week period retained GFP expression in hepatocytes (Fig 4F), and this was also most intense peri-portally (Fig 4E). Thus, before and early after the onset of liver injury, GFP was expressed by sinusoidal and bile ductular cells. However, with time, livers accumulated hepatocytic cells that expressed GFP. Such cells were apparent first in perivenular and midzonal areas (zones 3 and 2), but later accumulated predominately around portal tracts (i.e., in zone 1). During the 6 week time period of these experiments, the net numbers of GFP+ve cells (i.e., bile duct cells, sinusoidal cells and hepatocytes) increased significantly (Fig 4G), with hepatocytic cells accounting for the largest numbers of GFP+ve cells in mice that had recovered from MCDE diet-induced liver damage.

To clarify the origins of the GFP+ve hepatocytic cells that accumulated during the regeneration of injured livers, expression of Ki-67, an S phase marker, was assessed before, during and after liver injury (Fig 5A). Hepatocytes in healthy livers rarely expressed Ki-67, and did not up-regulate this proliferation marker during or after liver injury. Rare bile ductular cells in portal tracts were Ki-67+ve at baseline, but numbers of Ki-67+ve bile ductular cells did not change much during or after liver injury. In contrast, the numbers of sinusoidal cells expressing Ki-67 increased more than 10 fold in perivenular areas during liver injury and then returned to baseline with recovery. Ki-67+ve fibroblastic-appearing cells were easily demonstrated in liver sinusoids after 1 week of MCDE diet treatment (Fig 5B). Most of these cells co-expressed α-SMA, a marker of myofibroblastic HSC (Fig 5C). The number of α-SMA/Ki-67 double positive cells was more than 10 fold higher in the livers of mice that had received 1 week of MCDE diet treatment than in healthy mice, but quickly declined to basal levels (Fig 5D). Thus, liver injury induced a transient wave of proliferative activity in α-SMA+ve sinusoidal cells, and this preceded the accumulation of GFP-expressing hepatocytic cells. Together, these findings suggest that the GFP+ve hepatocytic cells may have been derived from the fibroblastic (i.e., α-SMA+ve) cells.

IHC was done to track α-SMA expression before, during, and after MCDE diet-induced liver injury (Suppl Fig 3). Before exposure to MCDE diets, control GFAP-Cre/GFP mice (Con) exhibited only rare α-SMA+ve cells in portal tracts. Liver sinusoids (which contained

GFAP+ve stellate cells, Fig 1) lacked α-SMA-expressing cells (Suppl Fig 3A-B). After 1 week treatment with MCDE diets, however, livers contained large numbers of α-SMA+ve cells, and these were localized predominately in perivenular and mid-zonal sinusoids. Occasional hepatocytic cells in zone 3 also expressed this marker (Suppl 3C). Because GFAP-expressing Q-HSC are an important source of the GFAP-negative/α-SMA+ve fibroblasts that accumulate in injured livers [21–23], livers were double immunostained to determine if these markers co-localized in the cells of GFAP-Cre/GFP mice (Fig 6A–B). As expected, numerous sinuosoidal cells that co-expressed GFP and α-SMA were noted in hepatic sinuosoids of mice that had been fed MCDE diets for one week. Scattered GFP/α–SMA double+ve hepatocytic cells were also evident. The latter were particularly prominent near clusters of double+ve sinusoidal cells and were also observed immediately adjacent to terminal hepatic venules. At this time point, these areas also harbored rare hepatocytic cells that expressed GFP, but not α-SMA, although the latter were much less prevalent than double+ve sinusoidal or hepatocytic cells. Over the course of the study, the numbers and lobular distribution of the GFP/α-SMA double+ve sinusoidal cells (Fig 6C) corresponded to that observed for α-SMA-expressing cells in general (Fig 5), peaking after 1 week of liver injury and then quickly declining to basal levels. Thus, MCDE diet -induced liver injury transiently expanded populations of GFP/α-SMA double+ve sinusoidal cells. This process was accompanied by the appearance of occasional GFP/α-SMA double+ve hepatocytic cells, and both events occurred weeks before large numbers of hepatocytic GFP-positive/α-SMA negative hepatocytic cells accumulated.

In aggregate, the IHC data support the concept that the accumulation of GFP+ve hepatocytic cells that occurred as MCDE diet-injured livers regenerated resulted from the differentiation of GFP/α-SMA double+ve sinusoidal cells. To investigate this possibility further, liver sections obtained before, during and after exposure to hepatotoxic diets were stained to demonstrate liver progenitor cell cytokeratins (Suppl Fig 4). Double immuno-staining was also done to determine if the GFP+ve hepatocytic cells that appeared early after the onset of liver injury co-expressed AE1/AE3-reactive cytokeratins that are known to exist in subpopulations of hepatic epithelial progenitors[45]. Occasional hepatocytic cells in zones 2–3 co-expressed GFP and hepatic progenitor cytokeratins after 1 week of treatment with MCDE diets (Fig 6D). Hence, early after the onset of liver injury in GFAP-Cre/GFP mice, GFP+ve hepatocytic cells that co-expressed α-sma and epithelial progenitor cell cytokeratins emerged. This event was transient and preceded the accumulation of large numbers of GFP(+) hepatocytic cells that lacked expression of either of the other markers. Because mature hepatocytes normally do not express either α-SMA or AE1/AE3-reactive cytokeratins, IHC was done to determine if the GFP(+) hepatocytic cells expressed albumin protein, a marker of mature hepatocytes. Livers were examined when the animals had completely recovered from their diet-induced liver injury (Fig 3), at a time when GFP(+) hepatocytic cells comprised almost one-third of the hepatic parenchyma (Fig 4). Virtually all of the GFP(+) hepatocytic cells co-expressed albumin at this time point (Fig 6E-G, confirming that restoration of liver mass (Fig 3) resulted from reconstitution of the liver by functioning mature hepatocytes.

Because the findings in MCDE-treated mice suggested that liver injury provoked Q-HSC to transition through a proliferative, myofibroblastic phase before differentiating into mature hepatocytes, we examined primary HSC for markers of hepatocyte progenitors and evidence of epithelial-mesenchymal transitions. QRT PCR analysis of RNA obtained from freshly isolated HSC revealed expression of classical markers for Q-HSC (GFAP and PPARγ, Fig 7A, B), as well as biliary epithelial cells (CK-19 and aquaporin-1, Fig 7C,D), immature hepatocytes (AFP, Fig 7H), and more primitive epithelial progenitors (mpk, NCAM, and CK7, Fig 7E–G). Thus, the gene expression profile of our Q-HSC suggested that these isolates were enriched with putative hepatocyte and cholangiocyte progenitors. During

standard culture conditions, these cells down-regulated their expression of GFAP and PPARγ (Fig 7A,B) and became myofibroblastic, up-regulating their expression of α-SMA and collagen I α1 (Fig 7I,J). The latter results are consistent with published data about gene expression changes that typically occur as wild type Q-HSC transition to MF-HSC [9, 46]. During HSC activation to a myofibroblastic phenotype, expression of S100A4 (also called fibroblast specific protein) (Fig 7K), a marker of epithelial-derived fibroblasts[47], increased, and expression of both biliary epithelial markers (Fig 7C, D) and markers of immature hepatocytes (Fig 7G,H) fell. Expression of mpk and NCAM (Fig 7E, F), markers of immature liver progenitors, increased concomitantly. Western blot analysis verified that changes in mRNA expression of representative stellate cell, mesenchymal and epithelial markers were accompanied by similar changes in protein content (Fig 7M). Throughout this process, primary HSC from GFAP-Cre/GFP mice retained GFP expression at both the mRNA and protein levels (Fig 7L, N, O), demonstrating that the activated HSC were progeny of Q-HSC that initially expressed GFAP.

Discussion

Our findings support the concept that HSC are capable of differentiating into hepatocytes. Published evidence had suggested this possibility, but definitive proof has been difficult to acquire in experimental animals [1618, 48, 49]. More direct evidence for this concept was provided by studies that cultured a subpopulation of HSC that had been enriched for cells expressing the mulipotent progenitor marker, CD133. Depending on the culture conditions, such cells were shown to generate various cell types, including myofibroblasts, cholangiocytes, and hepatocytes [1]. However, because primary HSC isolates were the source of the CD133(+) cells, it was impossible to exclude the possibility that differential outgrowth of rare cell types that contaminated the original preparation might have accounted for the findings. Earlier analyses of clonal lines that were derived from HSC that had been isolated from a single adult CCl4-treated rat [50] argue against cell contamination as an explanation for HSC heterogeneity. Different HSC clones from that rat exhibited variable co-expression of liver epithelial and mesenchymal markers. Moreover, clones that predominately expressed mesenchymal genes when cultured in media with a high serum content acquired the epithelial-predominant phenotype of other AFP/CK19 co-expressing clones when cultured in serum-depleted medium [7]. Although compelling, however, the findings in cell lines might merely have reflected changes that were acquired during the cloning process.

The fate mapping approach employed in the present study overcomes some of the inherent limitations of the earlier strategies that were used to characterize HSC. In rats, mice and humans, Q-HSC express GFAP and down-regulate this marker as they become myofibroblastic [21–23, 51]. By using GFAP promoter elements to regulate expression of Cre-recombinase in transgenic mice carrying floxed repressor elements that controlled expression of GFP or LacZ alleles, we were able to track the fate of Q-HSC during liver injury and regeneration. We confirmed that basal expression of various mesenchymal markers is negligible in Q-HSC. During both injury-related activation in mice, and "spontaneous" activation that occurs during culture on plastic dishes, HSC become highly proliferative and begin to co-express markers of mesenchyme and progenitors. In GFAP-Cre/GFP mice, these transitional cells disappeared as GFP-expressing hepatocytes emerged, and eventually the hepatocytic cells repopulated large areas of the hepatic parenchyma. Freshly isolated primary HSC expressed several epithelial genes and acquired a mesenchymal-type phenotype when we cultured them under standard conditions that are known to encourage myofibroblastic transformation and growth [11–13]. Another group has already demonstrated that primary HSC can differentiate into hepatocytes when they are

cultured with appropriate growth factors[1]. Hence, our new findings complement and extend earlier *in vitro* and *in vivo* evidence that HSC populations contain hepatocyte progenitors.

HSC also appear to be related to ductular cells. Although intermediate filament expression often varies over the course of cellular differentiation, qualitative differences in intermediate filaments are often used to differentiate cell types [52]. Others reported that both HSC and ductular cells express synemin[48], and the present study demonstrates that they also share expression of GFAP, which is another type of intermediate filament [53]. The similarities in intermediate filament sub-types that exist in HSC and ductular cells suggest that HSC and ductular cells may have a common lineage. This concept is supported by our observation that freshly isolated primary HSC also express several other biliary epithelial markers, such as CK-19, aquaporin-1, and CK7. Ductular cells have long been implicated as hepatocyte progenitors [54]. In livers injured by MCDE diets, however, ductular cell proliferation did not increase. Therefore, this cell population did not expand to replace hepatocytes and recover the liver mass that was lost during MCDE diet exposure. Sell and colleagues reported similar findings in allyl alcohol-treated rats, another model in which liver regeneration is accomplished by oval cells[18]. In healthy livers, oval cells are thought to reside along canals of Hering, the most proximal extensions of the biliary tree [55]. These cells are considered to be the adult equivalent of fetal hepatoblasts, i.e., bipotent hepatic progenitors that can differentiate into either hepatocytes or cholangiocytes [56, 57]. Thus, the heterogeneity of oval cell populations is thought to reflect the admixture of primitive oval cells and their progeny that are at various stages of differentiation [58]. Although our studies do not resolve whether or not Q-HSC are the progeny or precursors of ductular cells, they are clearly capable of generating hepatocytes. Therefore, HSC may belong to the oval cell family.

Some may consider the concept that HSC are a type of oval cell to be heretical. However, in addition to the literature that has already been discussed, there is actually considerable published data about fetal livers that also support this hypothesis. Liver epithelial cells and some HSC are both thought to originate from endoderm [59–61]. Fetal livers contain large numbers of bipotent hepatoblasts (oval cells), as well as cells that co-express liver epithelial and HSC markers (e.g., cytokeratins 7/8, desmin, and α-sma) [60]. Hence, the simplest hypothesis to explain all of our observations is that HSC are a type of oval cell, and in certain circumstances, these cells transition through a mesenchymal phase before differentiating into mature liver epithelial cells, including hepatocytes. This logic is appealing because it does not preclude the possibility that the cells may terminally differentiate into fibroblasts in other microenvironments. It also allows for the possibility that some epithelial progeny of HSC may be capable of undergoing epithelial-mesenchymal transition to reconstitute more fibroblastic populations, as was recently demonstrated in some hepatocytic cells that were cultured under pro-fibrogenic conditions [62], and in bile ductular cells in patients with primary biliary cirrhosis [63]. Viewed from this perspective, HSC appear positioned to dictate the ultimate outcome of liver injury, and efforts to differentiate mechanisms that promote their maturation into epithelial, as opposed to fibroblastic, cells have important clinical implications.

Supplementary Material

Refer to Web version on PubMed Central for supplementary material.

Acknowledgments

This work was supported in part by NIAAA 5R01- AA0 10154 (AMD), and VA Research Scholar Award and VA Merit Award (GDA)

References

1. Kordes C, Sawitza I, Muller-Marbach A, et al. CD133+ hepatic stellate cells are progenitor cells. Biochem Biophys Res Commun. 2007; 352:410–7. [PubMed: 17118341]
2. Niki T, Pekny M, Hellemans K, et al. Class VI intermediate filament protein nestin is induced during activation of rat hepatic stellate cells. Hepatology. 1999; 29:520–7. [PubMed: 9918930]
3. Fujio K, Evarts RP, Hu Z, et al. Expression of stem cell factor and its receptor, c-kit, during liver regeneration from putative stem cells in adult rat. Lab Invest. 1994; 70:511–6. [PubMed: 7513770]
4. Hu Z, Evarts RP, Fujio K, et al. Expression of hepatocyte growth factor and c-met genes during hepatic differentiation and liver development in the rat. Am J Pathol. 1993; 142:1823–30. [PubMed: 8506951]
5. Asahina K, Sato H, Yamasaki C, et al. Pleiotrophin/heparin-binding growth-associated molecule as a mitogen of rat hepatocytes and its role in regeneration and development of liver. Am J Pathol. 2002; 160:2191–205. [PubMed: 12057922]
6. Yoshino R, Miura K, Segawa D, et al. Epimorphin expression and stellate cell status in mouse liver injury. Hepatol Res. 2006; 34:238–49. [PubMed: 16480920]
7. Sicklick JK, Choi SS, Bustamante M, et al. Evidence for epithelial-mesenchymal transitions in adult liver cells. Am J Physiol Gastrointest Liver Physiol. 2006; 291:G575–83. [PubMed: 16710052]
8. Yang L, Wang Y, Mao H, et al. Sonic hedgehog is an autocrine viability factor for myofibroblastic hepatic stellate cells. J Hepatol. 2008; 48:98–106. [PubMed: 18022723]
9. Bataller R, Brenner DA. Hepatic stellate cells as a target for the treatment of liver fibrosis. Semin Liver Dis. 2001; 21:437–51. [PubMed: 11586471]
10. Gressner OA, Weiskirchen R, Gressner AM. Evolving concepts of liver fibrogenesis provide new diagnostic and therapeutic options. Compar Hepatol. 2007; 6:1–13.
11. Friedman SL, Roll FJ, Boyles J, et al. Hepatic lipocytes: the principal collagen-producing cells of normal rat liver. Proc Natl Acad Sci U S A. 1985; 82:8681–5. [PubMed: 3909149]
12. Kent G, Gay S, Inouye T, et al. Vitamin A-containing lipocytes and formation of type III collagen in liver injury. Proc Natl Acad Sci U S A. 1976; 73:3719–22. [PubMed: 1068482]
13. Maher JJ, McGuire RF. Extracellular matrix gene expression increases preferentially in rat lipocytes and sinusoidal endothelial cells during hepatic fibrosis in vivo. J Clin Invest. 1990; 86:1641–8. [PubMed: 2243137]
14. Reeves HL, Friedman SL. Activation of hepatic stellate cells--a key issue in liver fibrosis. Front Biosci. 2002; 7:d808–26. [PubMed: 11897564]
15. Rockey DC, Weisiger RA. Endothelin induced contractility of stellate cells from normal and cirrhotic rat liver: implications for regulation of portal pressure and resistance. Hepatology. 1996; 24:233–40. [PubMed: 8707268]
16. Roskams T. Different types of liver progenitor cells and their niches. J Hepatol. 2006; 45:1–4. [PubMed: 16723168]
17. Yin L, Lynch D, Ilic Z, et al. Proliferation and differentiation of ductular progenitor cells and littoral cells during the regeneration of the rat liver to CCl4/2-AAF injury. Histol Histopathol. 2002; 17:65–81. [PubMed: 11813887]
18. Yin L, Lynch D, Sell S. Participation of different cell types in the restitutive response of the rat liver to periportal injury induced by allyl alcohol. J Hepatol. 1999; 31:497–507. [PubMed: 10488710]
19. Libbrecht L, Cassiman D, Desmet V, et al. The correlation between portal myofibroblasts and development of intrahepatic bile ducts and arterial branches in human liver. Liver. 2002; 22:252–8. [PubMed: 12100576]
20. Omenetti A, Yang L, Li YX, et al. Hedgehog-mediated mesenchymal-epithelial interactions modulate hepatic response to bile duct ligation. Lab Invest. 2007; 87:499–514. [PubMed: 17334411]
21. Buniatian G, Hamprecht B, Gebhardt R. Glial fibrillary acidic protein as a marker of perisinusoidal stellate cells that can distinguish between the normal and myofibroblast-like phenotypes. Biol Cell. 1996; 87:65–73. [PubMed: 9004488]

22. Neubauer K, Knittel T, Aurisch S, et al. Glial fibrillary acidic protein--a cell type specific marker for Ito cells in vivo and in vitro. J Hepatol. 1996; 24:719–30. [PubMed: 8835748]
23. Geerts A, Niki T, Hellemans K, et al. Purification of rat hepatic stellate cells by side scatter-activated cell sorting. Hepatology. 1998; 27:590–8. [PubMed: 9462662]
24. Yokoi Y, Namihisa T, Kuroda H, et al. Immunocytochemical detection of desmin in fat-storing cells (Ito cells). Hepatology. 1984; 4:709–14. [PubMed: 6204917]
25. Buchholz M, Kestler HA, Holzmann K, et al. Transcriptome analysis of human hepatic and pancreatic stellate cells: organ-specific variations of a common transcriptional phenotype. J Mol Med. 2005; 83:795–805. [PubMed: 15976918]
26. Trim N, Morgan S, Evans M, et al. Hepatic stellate cells express the low affinity nerve growth factor receptor p75 and undergo apoptosis in response to nerve growth factor stimulation. Am J Pathol. 2000; 156:1235–43. [PubMed: 10751349]
27. Meurer SK, Tihaa L, Lahme B, et al. Identification of endoglin in rat hepatic stellate cells: new insights into transforming growth factor beta receptor signaling. J Biol Chem. 2005; 280:3078–87. [PubMed: 15537649]
28. Xu H, Cerrato F, Baldini A. Timed mutation and cell-fate mapping reveal reiterated roles of Tbx1 during embryogenesis, and a crucial function during segmentation of the pharyngeal system via regulation of endoderm expansion. Development. 2005; 132:4387–95. [PubMed: 16141220]
29. Eleazar JA, Memeo L, Jhang JS, et al. Progenitor cell expansion: an important source of hepatocyte regeneration in chronic hepatitis. J Hepatol. 2004; 41:983–91. [PubMed: 15582132]
30. Baumann U, Crosby HA, Ramani P, et al. Expression of the stem cell factor receptor c-kit in normal and diseased pediatric liver: identification of a human hepatic progenitor cell? Hepatology. 1999; 30:112–7. [PubMed: 10385646]
31. Roskams TA, Libbrecht L, Desmet VJ. Progenitor cells in diseased human liver. Semin Liver Dis. 2003; 23:385–96. [PubMed: 14722815]
32. Ip E, Farrell G, Hall P, et al. Administration of the potent PPARalpha agonist, Wy-14,643, reverses nutritional fibrosis and steatohepatitis in mice. Hepatology. 2004; 39:1286–96. [PubMed: 15122757]
33. Roskams T, Yang SQ, Koteish A, et al. Oxidative stress and oval cell accumulation in mice and humans with alcoholic and nonalcoholic fatty liver disease. Am J Pathol. 2003; 163:1301–11. [PubMed: 14507639]
34. Oben JA, Diehl AM. Sympathetic nervous system regulation of liver repair. Anat Rec A Discov Mol Cell Evol Biol. 2004; 280:874–83. [PubMed: 15382023]
35. Zhuo L, Theis M, Alvarez-Maya I, et al. hGFAP-cre transgenic mice for manipulation of glial and neuronal function in vivo. Genesis. 2001; 31:85–94. [PubMed: 11668683]
36. Mao X, Fujiwara Y, Chapdelaine A, et al. Activation of EGFP expression by Cre-mediated excision in a new ROSA26 reporter mouse strain. Blood. 2001; 97:324–6. [PubMed: 11133778]
37. Soriano P. Generalized lacZ expression with the ROSA26 Cre reporter strain. Nat Genet. 1999; 21:70–1. [PubMed: 9916792]
38. Hutterer F, Rubin E, Popper H. Mechanism Of Collagen Resorption In Reversible Hepatic Fibrosis. Exp Mol Pathol. 1964; 86:215–23. [PubMed: 14194321]
39. Tian YW, Smith PG, Yeoh GC. The oval-shaped cell as a candidate for a liver stem cell in embryonic, neonatal and precancerous liver: identification based on morphology and immunohistochemical staining for albumin and pyruvate kinase isoenzyme expression. Histochem Cell Biol. 1997; 107:243–50. [PubMed: 9105895]
40. George J, Pera N, Phung N, et al. Lipid peroxidation, stellate cell activation and hepatic fibrogenesis in a rat model of chronic steatohepatitis. J Hepatol. 2003; 39:756–64. [PubMed: 14568258]
41. Knight B, Yeap BB, Yeoh GC, et al. Inhibition of adult liver progenitor (oval) cell growth and viability by an agonist of the peroxisome proliferator activated receptor (PPAR) family member gamma, but not alpha or delta. Carcinogenesis. 2005; 26:1782–92. [PubMed: 15917308]
42. Knight B, Akhurst B, Matthews VB, et al. Attenuated liver progenitor (oval) cell and fibrogenic responses to the choline deficient, ethionine supplemented diet in the BALB/c inbred strain of mice. J Hepatol. 2007; 46:134–41. [PubMed: 17112626]

43. Yang L, Chan CC, Kwon OS, et al. Regulation of peroxisome proliferator-activated receptor-gamma in liver fibrosis. Am J Physiol Gastrointest Liver Physiol. 2006; 291:G902–11. [PubMed: 16798724]
44. Glaser SS, Rodgers RE, Phinizy JL, et al. Gastrin inhibits secretin-induced ductal secretion by interaction with specific receptors on rat cholangiocytes. Am J Physiol. 1997; 273:G1061–70. [PubMed: 9374703]
45. Vadlamani I, Brunt EM. Hepatocellular progenitor cell tumor of the gallbladder: a case report and review of the literature. Mod Pathol. 2005; 18:864–70. [PubMed: 15696116]
46. Miyahara T, Schrum L, Rippe R, et al. Peroxisome proliferator-activated receptors and hepatic stellate cell activation. J Biol Chem. 2000; 275:35715–22. [PubMed: 10969082]
47. Iwano M, Plieth D, Danoff TM, et al. Evidence that fibroblasts derive from epithelium during tissue fibrosis. J Clin Invest. 2002; 110:341–50. [PubMed: 12163453]
48. Schmitt-Graeff A, Jing R, Nitschke R, et al. Synemin expression is widespread in liver fibrosis and is induced in proliferating and malignant biliary epithelial cells. Hum Pathol. 2006; 37:1200–10. [PubMed: 16938526]
49. Koenig S, Probst I, Becker H, et al. Zonal hierarchy of differentiation markers and nestin expression during oval cell mediated rat liver regeneration. Histochem Cell Biol. 2006; 126:723–34. [PubMed: 16835754]
50. Greenwel P, Schwartz M, Rosas M, et al. Characterization of fat-storing cell lines derived from normal and CCl4-cirrhotic livers. Differences in the production of interleukin-6. Lab Invest. 1991; 65:644–53. [PubMed: 1753710]
51. Xu L, Hui AY, Albanis E, et al. Human hepatic stellate cell lines, LX-1 and LX-2: new tools for analysis of hepatic fibrosis. Gut. 2005; 54:142–51. [PubMed: 15591520]
52. Omary MB, Coulombe PA, McLean WH. Intermediate filament proteins and their associated diseases. N Engl J Med. 2004; 351:2087–100. [PubMed: 15537907]
53. McCall MA, Gregg RG, Behringer RR, et al. Targeted deletion in astrocyte intermediate filament (Gfap) alters neuronal physiology. Proc Natl Acad Sci U S A. 1996; 93:6361–6. [PubMed: 8692820]
54. Alison MR, Golding MH, Sarraf CE. Pluripotential liver stem cells: facultative stem cells located in the biliary tree. Cell Prolif. 1996; 29:373–402. [PubMed: 8883463]
55. Libbrecht L, Roskams T. Hepatic progenitor cells in human liver diseases. Semin Cell Dev Biol. 2002; 13:389–96. [PubMed: 12468238]
56. Lemire JM, Shiojiri N, Fausto N. Oval cell proliferation and the origin of small hepatocytes in liver injury induced by D-galactosamine. Am J Pathol. 1991; 139:535–52. [PubMed: 1716045]
57. Dabeva MD, Shafritz DA. Activation, proliferation, and differentiation of progenitor cells into hepatocytes in the D-galactosamine model of liver regeneration. Am J Pathol. 1993; 143:1606–20. [PubMed: 7504886]
58. Thorgeirsson SS, Evarts RP, Bisgaard HC, et al. Hepatic stem cell compartment: activation and lineage commitment. Proc Soc Exp Biol Med. 1993; 204:253–60. [PubMed: 7694304]
59. Kiassov AP, Van Eyken P, van Pelt JF, et al. Desmin expressing nonhematopoietic liver cells during rat liver development: an immunohistochemical and morphometric study. Differentiation. 1995; 59:253–8. [PubMed: 8575647]
60. Suskind DL, Muench MO. Searching for common stem cells of the hepatic and hematopoietic systems in the human fetal liver: CD34+ cytokeratin 7/8+ cells express markers for stellate cells. J Hepatol. 2004; 40:261–8. [PubMed: 14739097]
61. Vassy J, Rigaut JP, Briane D, et al. Confocal microscopy immunofluorescence localization of desmin and other intermediate filament proteins in fetal rat livers. Hepatology. 1993; 17:293–300. [PubMed: 7679087]
62. Kaimori A, Potter J, Kaimori JY, et al. Transforming growth factor-beta1 induces an epithelial-to-mesenchymal transition state in mouse hepatocytes in vitro. J Biol Chem. 2007; 282:22089–101. [PubMed: 17513865]
63. Robertson H, Kirby JA, Yip WW, et al. Biliary epithelial-mesenchymal transition in posttransplantation recurrence of primary biliary cirrhosis. Hepatology. 2007; 45:977–81. [PubMed: 17393507]

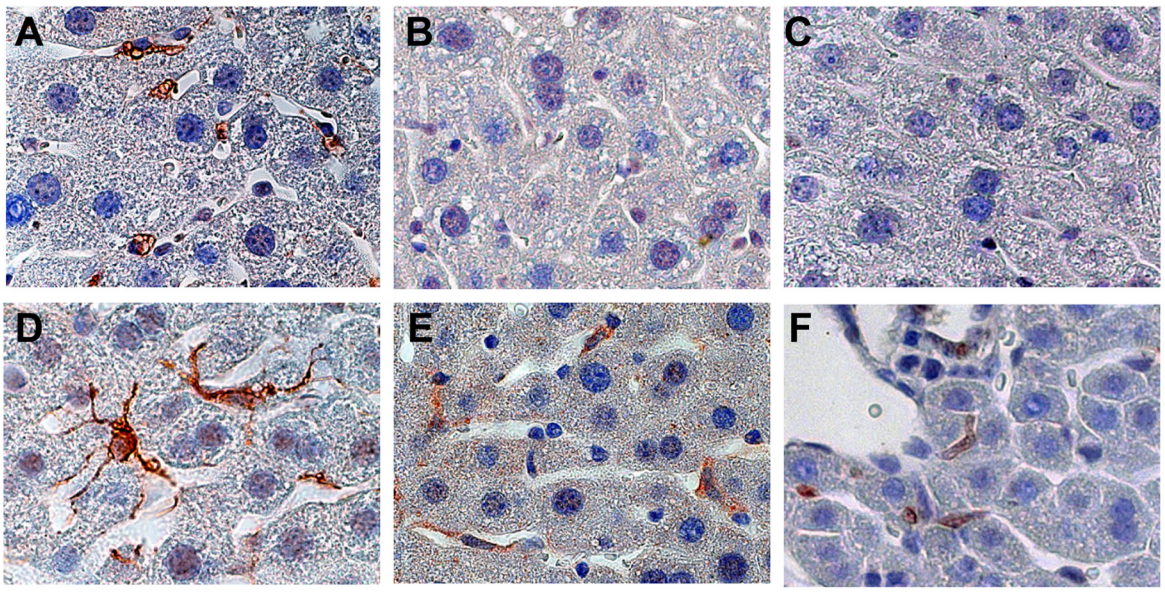

Figure 1. GFAP, Cre-recombinase and GFP expression in HSC of control and GFAP-Cre/reporter mice

Immunohistochemistry for GFAP (A,D), Cre-recombinase (B, E) and GFP (C,F) were performed in representative control (Ctr) (A–C) and GFAP-Cre/GFP (TG) mice (D–F). GFAP is expressed by hepatic stellate cells (HSC) in a representative Ctr mouse (A) and a representative GFAP-Cre/GFP (TG) mouse (D). HSC express Cre recombinase (E) and GFP (F) in TG mice, not in Ctr mice (B,C). (X100)

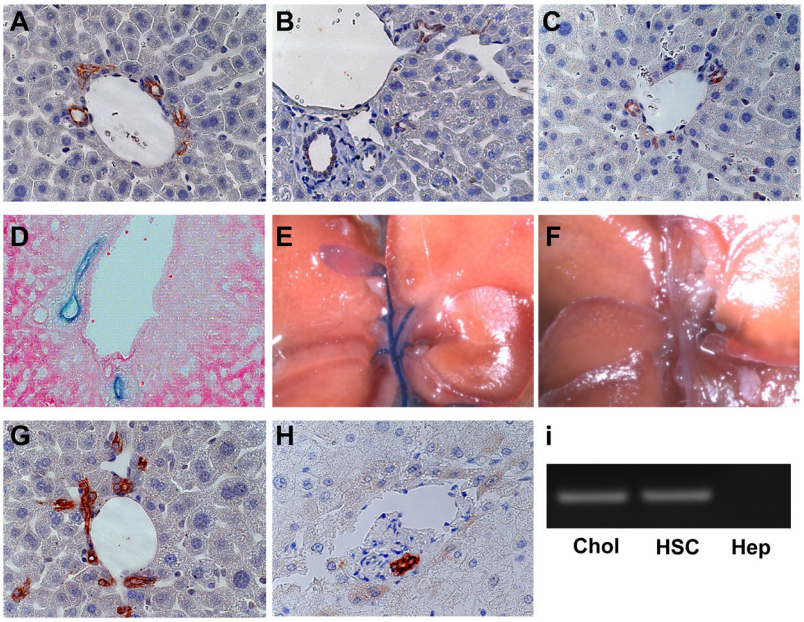

Figure 2. GFAP, Cre-recombinase and GFP expression in cholangiocytes of GFAP-Cre/reporter mice

GFAP (A), Cre-recombinase (B) and GFP (C) are expressed by bile ductular cells in portal triads of a representative GFAP-Cre/GFP (TG) mouse. Eosin-counterstained liver section from a representative GFAP-Cre/LacZ mouse showing LacZ(+) bile ductular cells (D). Extra-hepatic bile ducts, cystic duct and gallbladder exhibit β-galactosidase activity in a representative GFAP-Cre/LacZ mouse (E), but not in a Ctr mouse (F). Bile ductular cells in healthy adult mice (G) and a typical sample of non-diseased human liver (H) also express GFAP. Primary rat cholangiocytes (Chol) and HSC express GFAP mRNA, but primary hepatocytes (Hep) do not (I). (X63)

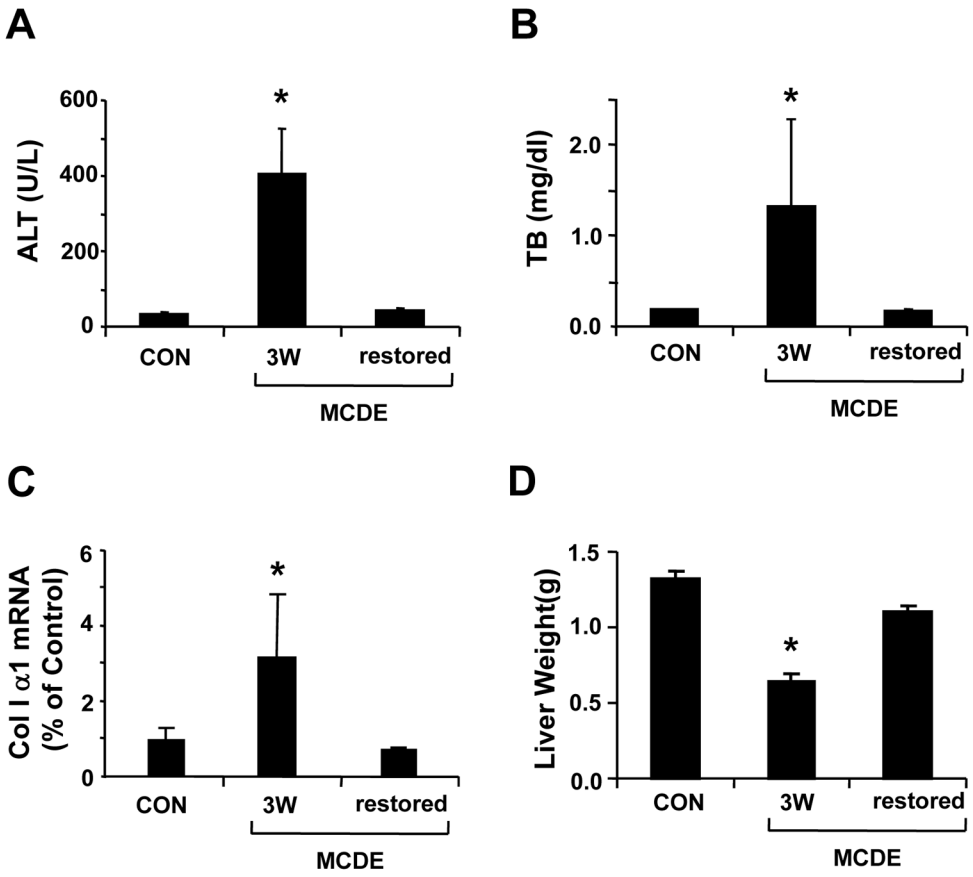

Figure 3. Effect of MCDE diet on serum liver enzymes levels, liver collagen I α1 mRNA and liver mass

Serum alanine aminotransferase (ALT) (A) and total bilirubin (TB) (B) levels were measured in controls (CON), mice fed MCDE diets for 3 weeks (MCDE 3W) and mice fed MCDE diets for 3 weeks and then returned to normal chow for 3 weeks before sacrifice (MCDE restored) (n=4 mice/group/time point). Collagen I α 1mRNA expression was evaluated in liver samples from the same mice using real time PCR (C). (D) Liver weight in the control and both MCDE diet fed groups (*P< 0.05 compared to control mice, n=4 mice/group/time point).

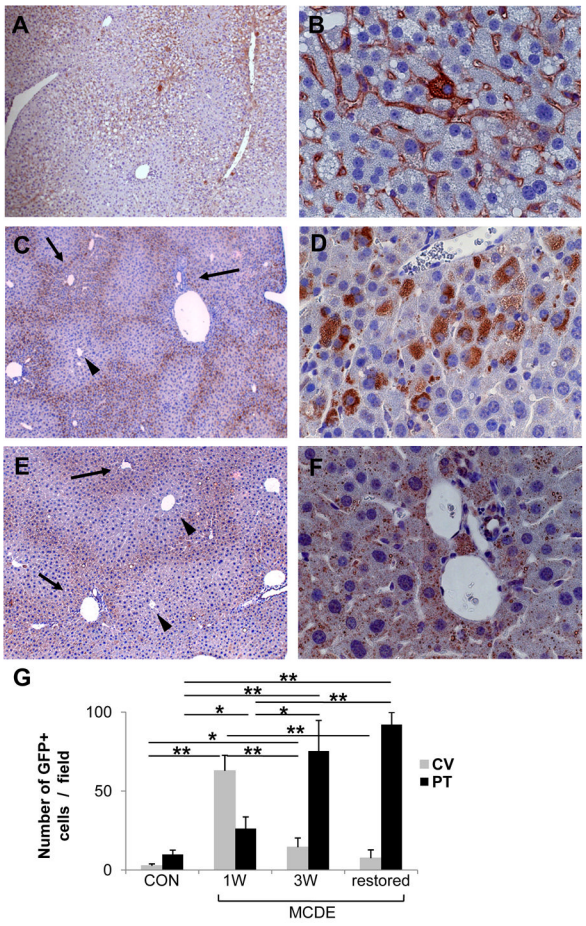

Figure 4. GFP expression in the livers of TG mice after injury

GFAP-Cre/GFP mice (n = 15) were fed MCDE-diets and survivors were sacrificed after 1 week (n = 4) or 3 weeks (n = 4). Other mice that survived 3 weeks of MCDE treatment (n = 4) were sacrificed after being switched back to normal diets for 3 weeks. GFP expression was assessed by immunohistochemistry. Representative results in mice that were sacrificed at the end of 1 week MCDE diet treatment (A, B), 3 weeks MCDE treatment (C, D), or 3 weeks after stopping a 3 week course of MDCE diets (E, F). Numbers of GFP-positive cells visualized at X40 were counted in different parts of the liver lobule (i.e., near central veins (CV) and portal tracts (PT)) (G). * < p 0.05, ** p < 0.005 (A, C, E original magnification X10; B, D, F X63). Arrows and arrowhead indicate portal triads and central veins, respectively.

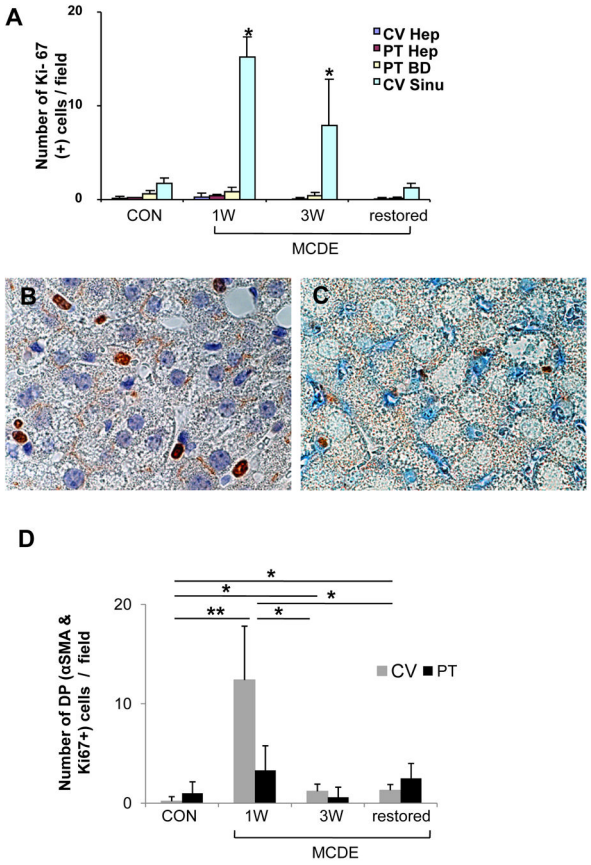

Figure 5. Ki-67 expression in the livers of TG mice

GFAP-Cre/GFP mice (n = 15) were fed MCDE-diets and survivors were sacrificed as described above (n = 4/group/time point). Immunohistochemistry for Ki-67 or double-immunohistochemistry for Ki-67/αSMA was performed. Numbers of Ki-67-positive cells visualized at X63 (high power) were counted in different parts of the liver lobule (i.e., near central veins (CV) and portal tracts (PT)) and in different cell types (i.e., hepatocytes (Hep), bile ductular cells (BD), and perisinuosoidal lining cells (Sinu)). Results are graphed as numbers of positive cells/field in (A).* $p < 0.05$ Ki-67 expression (B) and Ki-67 and αSMA co-expression (C) in mice that were sacrificed at the end of 1 week MCDE treatment. Numbers of double positive (DP) cells for Ki-67and αSMA in different areas of the liver lobule (CV or PT) were counted at different time points and results are graphed in (D). * $p < 0.05$, ** $p < 0.005$ (A, C magnification X100)

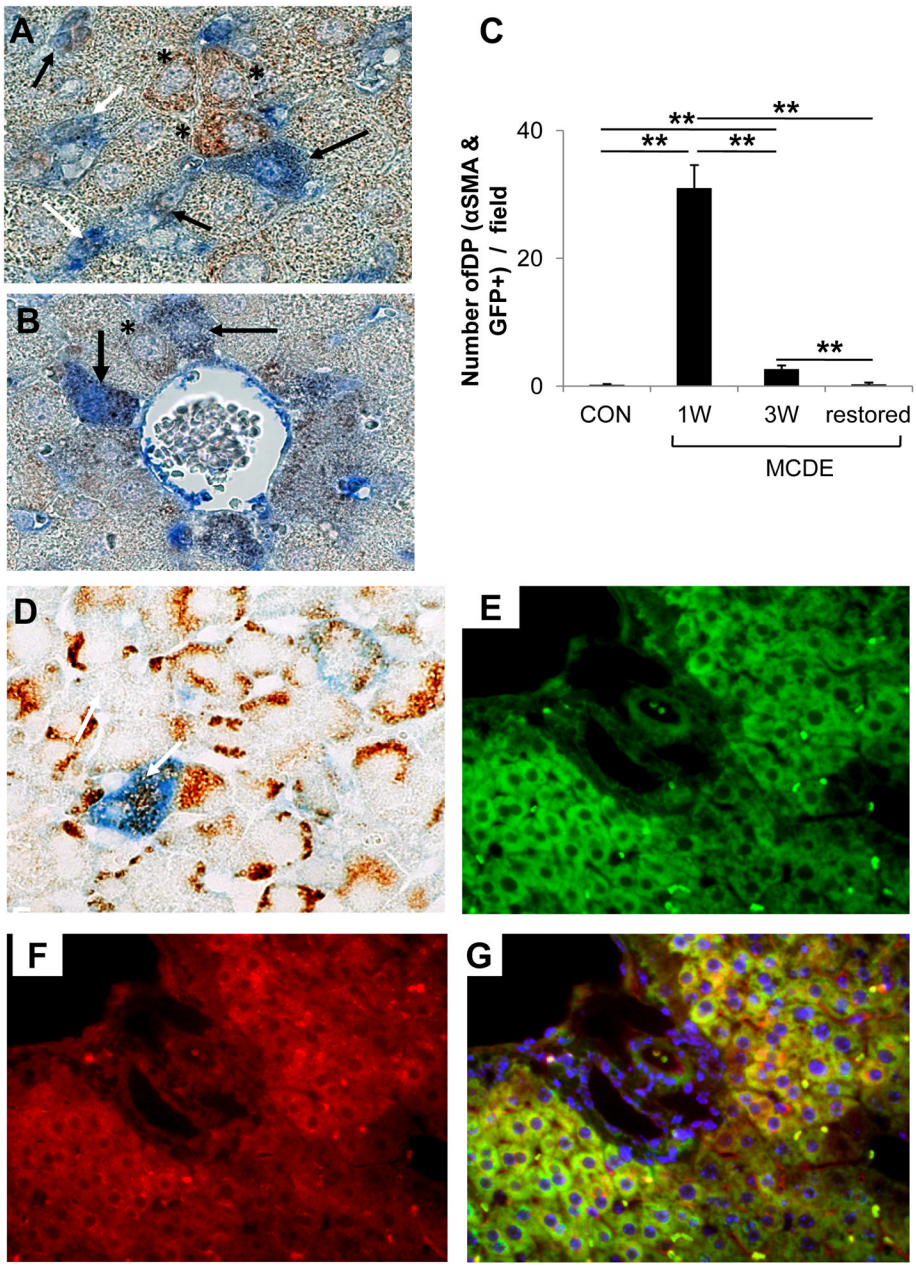

Figure 6. Co-expression of GFP with αSMA, AE1/3 or albumin in the livers of TG mice after liver injury

GFAP-Cre/GFP mice (n = 15) were fed MCDE-diets and survivors were sacrificed as described above (n = 4/group/time point). Double immunohistochemistry for GFP and αSMA (A–B) or AE1/3 (D) in the 1 week MCDE diet group. Numbers of double positive (DP) cells for GFP and αSMA in different areas were counted at different time points and results are graphed in (C). * $p < 0.05$, ** $p < 0.005$. Co-staining for GFP (E), Albumin (F), and a merged photomicrograph demonstrating co-expression of these markers (G) in a representative mouse that was switched from MCDE-diet to normal chow for 3 weeks. (A, B, D X100; E–G original magnification X63)

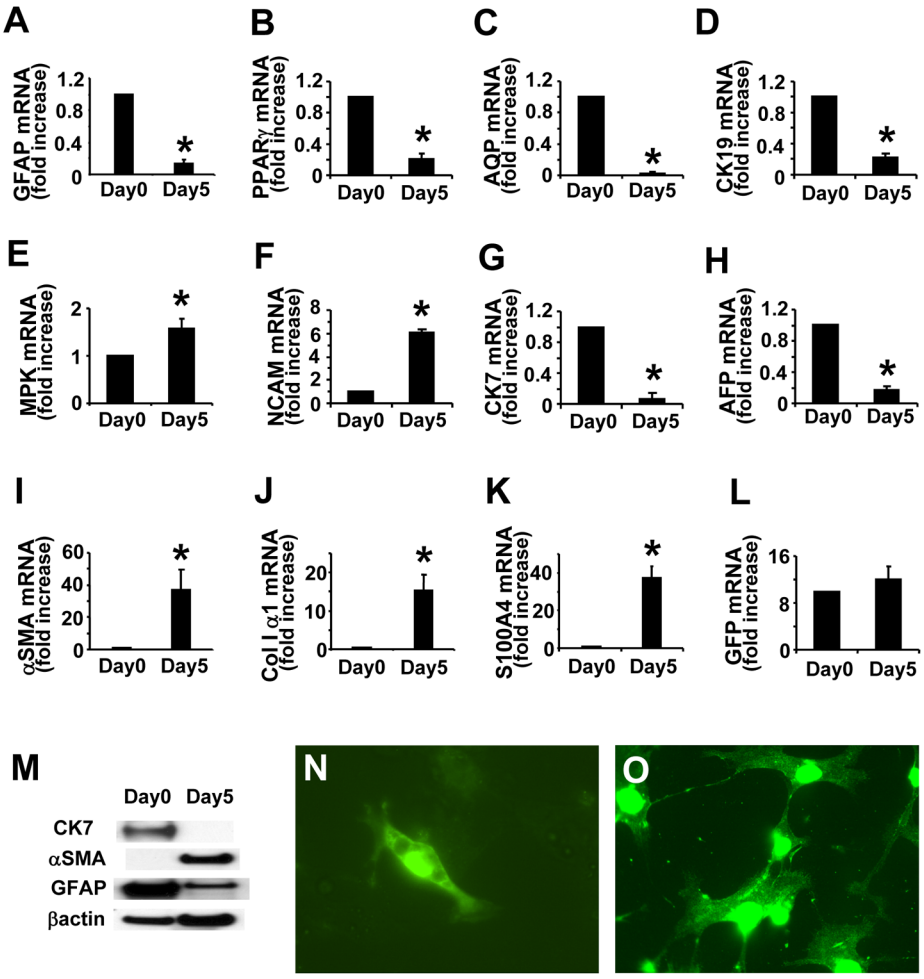

Figure 7. GFP expression in HSC from GFAP-cre/GFP mice

Analysis of gene expression by freshly isolated and 5 day culture-activated primary HSC from adult mice. Realtime RT-PCR was used to evaluated GFAP (A), PPARγ (B), aquaporin-1 (AQP) (C), CK-19 (D), MPK (E), NCAM (F), CK-7 (G), AFP (H),α-SMA (I), collagen I α1 (J), S100A4 (K), and GFP (L) mRNA levels. Western blot analysis for CK-7, αSMA and GFAP (M). Cultures of HSC were stained with anti-GFP antibody on day 0 (N) and day 5 (O). (Original magnification X63, *$p < 0.05$ vs day 0)